J Mater Sci (2011) 46:6975–6980
DOI 10.1007/s10853-011-5665-7

Preparation, characterization, and fluorescence properties of well-dispersed core–shell CdS/carbon nanoparticles

Kejie Zhang · Xiaoheng Liu · Yuxi Sun · Fei Wang

Received: 2 May 2011 / Accepted: 27 May 2011 / Published online: 10 June 2011

Abstract The core–shell CdS-carbon (CdS/C) nanoparticles were synthesized for the first time via a facile pyrolysis approach of bis(β-mercaptoethanol)-cadmium(II) as a single-source precursor. After using acid treatment method, well-dispersed and homogeneous core–shell CdS/C nanoparticles were obtained. The morphology, structure, and properties of CdS/C nanoparticles were investigated by X-ray diffraction (XRD), Raman spectra, transmission electron microscopy, X-ray photoelectron spectroscopy (XPS), and fluorescence spectroscopy. Most of the prepared nanoparticles presented core–shell structures with core diameter of $\sim$10 nm and shell thickness of $\sim$4 nm. The CdS core belonged to hexagonal crystal system. The carbon shell was employed as a good dispersion medium to form well-dispersed small sized CdS particles. XRD and XPS results revealed that there is an interaction between CdS core and carbon shell. Fluorescence measurement showed that the monodispersed CdS-carbon nanoparticles exhibit remarkable fluorescence enhancement effect compared with that of the pristine CdS nanoparticles, which indicates the prepared nanoparticles are a promising photoresponsive material.

Introduction

Surface functionalization has been recognized as an advanced and convincing method to tailor the properties of nanomaterials [1–11]. Surface coatings on nanostructure semiconductors can alter the charge, functionality, as well as the reactivity of materials, and consequently enhance the functional properties [1, 3, 12]. Designing core–shell structure is regarded as an effective surface coating method. Core–shell nanostructure semiconductors are comprised of at least one semiconductor nanoparticle which may serve as core or shell, such as Pt/CdS, Si/CdSe, CdS/ZnS, CdS/ZnO, Cr_2O_3/C, and so on. The chemical and physical properties of these materials depend on the choice of the two components. For example, a narrow band gap semiconductor nanoparticle can be capped with a wide gap material to prevent the formation of surface traps, leading to enhanced band edge luminescence in the core–shell system [12]. In addition, a protective shell material can be chosen to improve the chemical stability of the core and to maintain its performance for a long time, which is important for solar cells [1] and electrode materials of the Li-ion batteries [3].

In general, the conventional method to fabricate core–shell semiconductor nanoparticles, by encapsulating the core surfaces with a shell of desired material, requires multi-step processes. For examples, Pt/CdS [13], CdSe/CdS [14], CdS/ZnO [15], and CdS/S [16] were prepared by a two-step method while Fe_3O_4/C [17], SnO_2/C [18], CdS/ZnS [19], CdTe/CdS [20], and CdS/ZnS [21] were synthesized by a three-step method. All of the mentioned methods were carried out in liquid phase. Up to now, few researches have adopted the conventional solid pyrolysis technique to prepare core–shell materials. The main reason is that the products obtained by the method are usually sintered together making the uncontrollable particle-sizes. Although some improved pyrolysis methods such as metallorganic chemical vapor deposition [22], aerosol-assisted chemical vapor deposition [23], and atmospheric pressure chemical vapor deposition [24] have been applied to

K. Zhang · X. Liu (✉) · Y. Sun · F. Wang
Key Laboratory for Soft Chemistry and Functional Materials, Nanjing University of Science and Technology, Ministry of Education, Nanjing 210094, China
e-mail: xhliu@mail.njust.edu.cn

fabricate core–shell nanomaterials, it is still a key research challenge work to improve the conventional pyrolysis method.

As an important narrow bandgap semiconductor, CdS has many commercial applications such as optical detectors, light-emitting diodes, optoelectronic devices, and electrochemiluminescence [19, 25–27]. Previous results have demonstrated that the CdS nanoparticles play an important role in presenting their attractive physical properties, so that they have been widely used in the preparation of various nanostructural composites [27–29]. Carbon is a versatile coating material due to its chemical stability, biocompatibility, and possibility of surface modification. Although many efforts have been made to synthesize carbon-based CdS composites, such as carbon nanotube/CdS, CdS/graphene, spherical C/CdS, and CdS/carbon nanotube in liquid solvents using two or more materials [5, 26, 30–32], there are few studies on the preparation of core–shell CdS/carbon (CdS/C) nanoparticles by conventional pyrolysis of a single precursor in solid phase.

In this study, the bis(β-mercaptoethanol)-cadmium(II) ($Cd(SCH_2CH_2OH)_2$) was employed as the single-source precursor for the synthesis of sintered CdS/C nanomaterial by one-step conventional pyrolysis process. After acid treatment process, well-dispersed and homogeneous core–shell CdS/C nanoparticles were obained. The product presents remarkable fluorescence enhancement effects compared with pristine CdS nanoparticles.

Experimental section

Preparation of CdS/C nanoparticles

All the chemicals and reagents were of analytical purity and used as received without further purification. $Cd(SCH_2CH_2OH)_2$ ($Cd(MCE)_2$) was prepared by the method described previously [33]. In a typical process, $Cd(MCE)_2$ was heated directly in a horizontal muffle furnace from room temperature to 400 °C and kept at this temperature in N_2 for 2 h. Consequently, the mixture of CdS/C nanoparticles and uncoated CdS particles was obtained, which was named as "sintered sample." The sintered sample consisted of orange and black particles was immersed in hydrochloride acid aqueous solution (HCl, volume fraction: 12%) for 30 min. After filtration, the black colloid precipitates (namely acid-treated sample) were collected while the orange particles disappeared. For comparison, the pristine CdS nanoparticles with a diameter of ~10 nm were prepared by conventional chemical deposition method.

Characterization of the nanoparticles

X-ray diffraction (XRD), Raman spectra (RS), transmission electron microscopy (TEM), X-ray photoelectron spectroscopy (XPS), and room temperature photoluminescence (PL) spectroscopy were used to characterize the as-prepared nanocomposites. XRD was recorded on a Bruker D8 Advanced X-ray diffractometer using Cu Kα radiation ($\lambda = 1.54056$ Å) at 40 kV/40 mA. FT–RS were obtained with a Renishaw inVia Raman microscope with 514.5 nm provided by an Ar^+ laser. TEM and HRTEM were performed with a JEM-2100 microscope (JEOL) operating at 200 kV accelerating voltage. Samples were prepared as follows: disperse the products in ethanol by ultrasonication and place a drop of the suspension on a copper grid coated with an amorphous carbon film, and the ethanol was evaporated naturally. Images were acquired digitally on a scanning CCD camera. The composition analysis and the electronic binding energy were examined on an X-ray photoelectron spectroscope (Thermo ESCALAB 250), with AlKα (1486.7 eV) radiation for excitation (15 kV and 10 mA). The X-ray source was operated at 150 W. The C1s peak at a binding energy 284.7 eV was taken as an internal standard. PL spectra were obtained on a Cary Eclipse fluorescence spectrophotometer with a Xe lamp as the excitation light source.

Results and discussion

X-ray diffraction patterns are shown in Fig. 1. The diffraction peaks (in Fig. 1a) could be readily indexed to hexagonal CdS (space group: *P63mc*, $a = 4.136$ Å, $c = 6.713$ Å, $\alpha = \beta = 90°$, $\gamma = 120°$ and JCPDS No. 06-0314). As seen from Fig. 1, the broader Bragg peaks' positions of the acid-treated sample (b) are similar to the ones of the sintered sample (a), indicating coated CdS also pertained to hexagonal crystalloid. The peaks' intensity of the acid-treated sample is weaker than that of the sintered sample, implying some uncoated CdS crystals with high crystallinity were removed by the acid-treated approach. Another possible reason is that the surface of CdS core was coated by the protective carbon shell, which hindered the detection of coated CdS crystals. The positions of the diffraction peaks of the acid-treated sample also illuminated that coated CdS crystals with smaller sizes still survived after the acid-treated process, and the broadly diffused peak at 20°–30° is ascribed to carbon shell [34]. The inset is the part of the full figure (from 24° to 30°). Comparing with that of the sintered sample (a), the positions of diffraction peaks (shown with the vertical lines) of the acid-treated sample (b) make a slight shift to smaller coordinate numbers along the horizontal axis, which

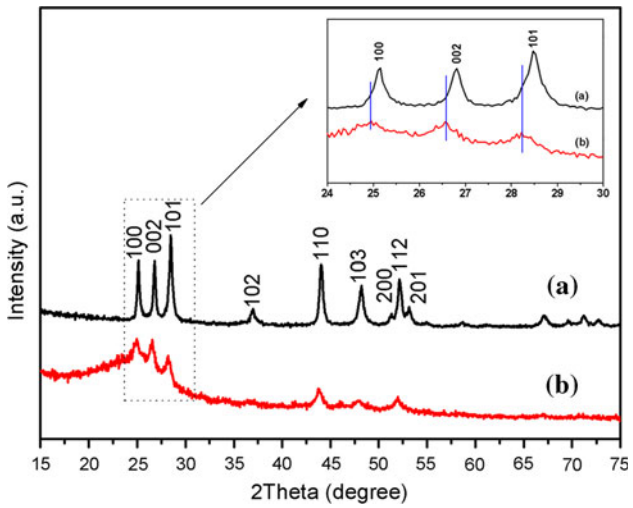

Fig. 1 XRD patterns of the sintered sample (*a*) and the acid-treated sample (*b*); the *inset* is the part of the full figure (from 24° to 30°)

implies the interplanar distance of coated CdS is larger than that of the sintered sample. The possible reason is that C shell afforded electrons to Cd atom, which weakened the binding energy and reduced the electrostatic attraction between Cd atom and S atom, resulting in the interplanar space becoming larger than that of pristine CdS. The ratiocination is consistent with XPS result. This phenomenon offered an evidence of the presence of CdS/C nanomaterial.

Figure 2 depicts the room temperature RS of the sintered product and the acid-treated sample. The Raman spectrum of the sintered product (a) displays two peaks at ~295 and ~591 cm^{-1}, which individually corresponds to the first- and second-order longitudinal optical (LO) phonon modes of CdS nanoparticles [35]. In addition, there are two Raman peaks at ~1344 and ~1581 cm^{-1}, corresponding to the D and G peaks of carbon [36], respectively. Compared with the sintered product, the acid-treated sample (b) only shows the D and G peaks of carbon, and no peaks of CdS, which implies that uncoated CdS particles are removed by HCl; and the CdS nanoparticles in the acid-treated sample are completely coated. This provides additional evidence of the existence of CdS/C nanomaterial.

Figure 3a, b display TEM images of core–shell CdS/carbon nanoparticles, which are highly monodispersed and homogeneous, scale bar, 100 and 20 nm, respectively. Figure 3c is the HRTEM image of a CdS/C nanoparticle with a core diameter of ~10 nm and a shell thickness of

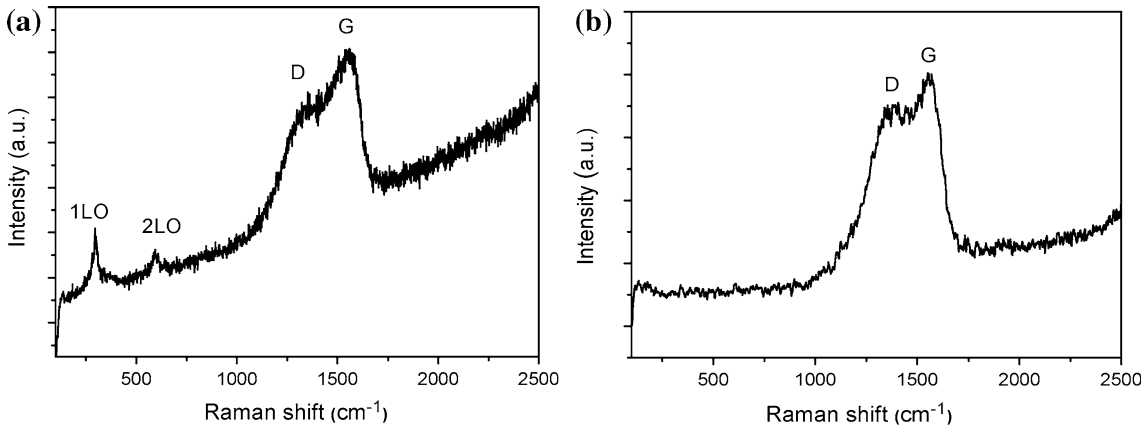

Fig. 2 Raman spectra of the sintered sample (*a*) and acid-treated sample (*b*)

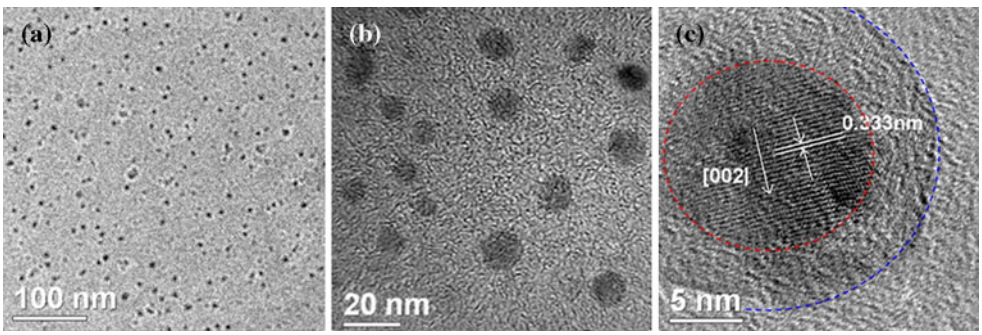

Fig. 3 TEM images: the acid-treated sample (**a**, **b**; *scale bar* 100 and 20 nm); HRTEM image of a core–shell CdS/C nanoparticle (**c**), *scale bar* 5 nm; the *dashed lines* are guides for eyes, distinguishing the core and shell boundaries, respectively

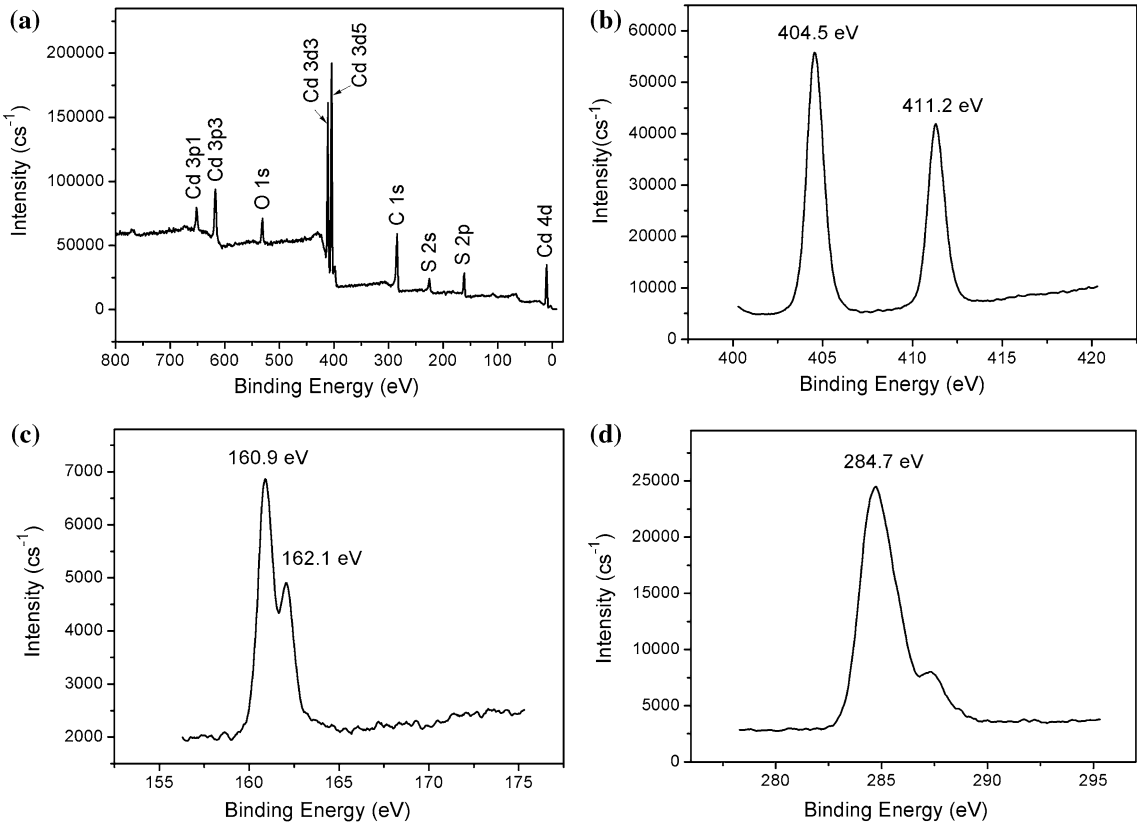

Fig. 4 Full XPS spectrum obtained from the surface of the acid-treated sample (**a**); narrow-scan XPS spectra of Cd 3d (**b**), S 2p (**c**), and C1s (**d**) from the sample (**a**)

~4 nm. Scale bar is 5 nm. The dashed lines are guides for eyes to distinguish the CdS core and carbon shell boundaries, respectively. According to the Bragg equation, the growth direction of CdS crystal is along the [002] direction. These CdS/C nanoparticles could retain a stable structure even after being heated at 400 °C for 10 h.

The XPS survey spectrum of the acid-treated sample is shown in Fig. 4. The identified peaks are labeled to the various corresponding elements. Figure 4a shows the full XPS spectrum taken from the surface of CdS/C nanoparticles. The peaks in the XPS data (Fig. 4a) could be identified to originate from Cd, S, C, and O elements. The O peaks stemmed from the atmospheric contamination. The binding energies obtained in the XPS analysis were corrected in consideration of the specimen charging and by referring to O1s at 530.7 eV. In the high resolution XPS spectrum of the CdS/C nanoparticles, the binding energies of Cd 3d doublet are located at 404.5 and 411.2 eV, respectively with a peak separation of 6.7 eV (Fig. 4b). Similarly, the peak position of S 2p is located at 160.9 and 162.1 eV (Fig. 4c); however, the separation is very small (~1.1 eV). It can be noticed that there is a slight shift in the Cd 3d peaks (from 405.5 to 404.5 eV, 412.2 to 411.2 eV) and S 2p peaks (165–160.9 eV) to lower binding energy comparing with their standard values reported in the literature for CdS [37–39]. A possible reason is that the Cd atoms are afforded the electrons from the carbon shell, which causes the electron density around Cd atoms to increase and the strength of the CdS bond to decrease [38]. Therefore, the binding energies of Cd 3d and S 2p are reduced. It is evident that there is an interaction between carbon shell and CdS nanoparticles, which agrees with XRD results. Figure 4d shows that the peak position of C1s is located at 284.7 eV. As the shell, carbon weakens the photosensitivity of coated CdS nanoparticles and passivated their surface [40], which might make CdS/C a novel electrode material in solar cells or optical detectors.

Figure 5 illustrates schematically the formation process conducted in N_2 atmosphere. In the first stage, $Cd(MCE)_2$ was thermally decomposed, forming CdS nanoparticles and the ligand fragments. Parts of the CdS nanoparticles were fully coated with the fragments. Further pyrolysis resulted in the formation of carbon shells, which could restrain coated CdS particles growth. The part coated or uncoated CdS particles grew up to a larger size when the reaction mixture was maintained at a higher temperature. Finally the coated and uncoated particles were sintered, forming a larger hardened sample. When the sample was treated by

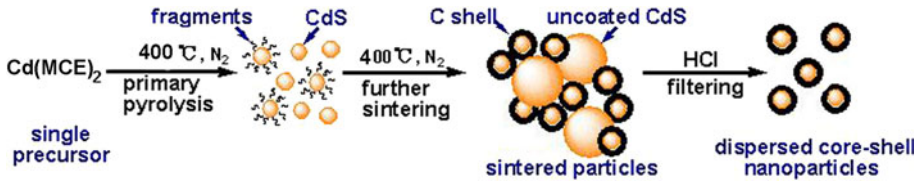

Fig. 5 A schematic diagram of the formation process of dispersed CdS/C nanoparticles obtained from pyrolysis of $Cd(MCE)_2$

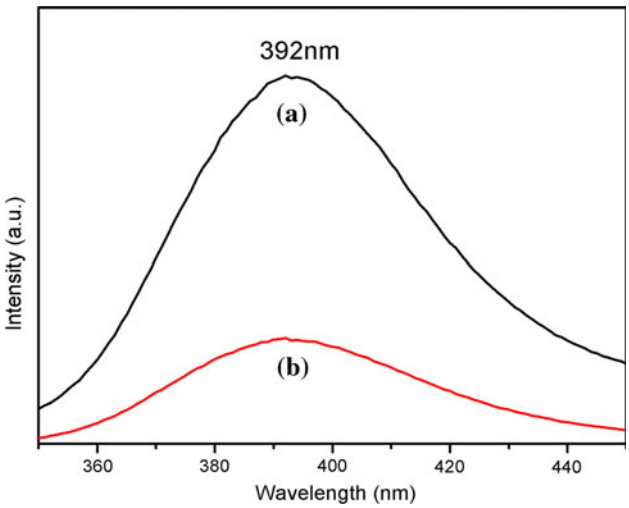

Fig. 6 Fluorescence spectra of the acid-treated sample (**a**) and the pristine CdS (**b**)

hydrochloride acid aqueous solution, the uncoated CdS particles were dissolved in the solution, resulting in the disintegration of the sintered sample and the formation of monodispersed CdS/C core–shell nanoparticles.

The room temperature solid-state PL fluorescence (exited with 320 nm laser) measurement results are shown in Fig. 6. The results of fluorescence spectra of the acid-treated sample (a) and the pristine CdS (b) showed a strong emission band at $\sim$392 nm. The characteristic emission band is ascribed to CdS excimer band-to-band emission [41], which obviously blue-shifted in comparison to that of the bulk CdS (512 nm) [42]. This blue-shifted phenomenon was mainly caused by quantum confinement of CdS nanoparticles [43]. The fluorescence intensity of the acid-treated sample is enhanced $\sim$3.5 times to that of the pristine CdS nanoparticles. The possible reason is that C shell effectively passivated the surface of CdS nanoparticles, and reduced their surface defects and nonradiative transition, which resulted in the fluorescence enhancement of as-prepared sample [40]. In other words, compared with ordinary loading, this coating action of carbon shell to CdS nanoparticles increased the contact between carbon and CdS, prevented the aggregation of coated CdS nanoparticles and passivated the surface of coated CdS nanoparticles, which were consistent with the results of XRD, TEM, and XPS. All of the above may make Cd/C nanoparticles demonstrate obvious fluorescence enhancement effect compared with the pristine CdS nanoparticles. Furthermore, carbon shell reduced the toxicity of coated CdS to enhance its biocompatibility, which could be used as fluorescent probes in biological labeling.

Conclusions

This study demonstrates the preparation of core–shell CdS/carbon nanoparticles from conventional pyrolysis of $Cd(SCH_2CH_2OH)_2$ in nitrogen without additional source. The uncoated CdS particles were removed by acid-treated process, and well-dispersed core–shell CdS/carbon nanoparticles were obtained. Individual CdS-carbon nanoparticle had a core diameter of $\sim$10 nm and a shell thickness of $\sim$4 nm. Carbon shell was a good dispersion medium to form well-dispersed and small CdS particles. XRD and XPS results implied that there was an interaction between core CdS and carbon shell. This might be the main reason that Cd/C nanoparticles presented obvious fluorescence enhancement effect compared with the pristine CdS nanoparticles, which could be useful in the design of luminescence and optoelectronic devices. Furthermore, this simple approach is desirable for synthesis of other carbon-based core–shell nanoparticles or other interesting nanostructures, since our studies show that the method is also feasible to prepare ZnS/C, CuS/C, and NiS/C nanocomposites, which is now being investigated.

Acknowledgements This project is supported financially by the Natural Science Foundation of China (Grant No. 20974045) and the Natural Science Foundation of Jiangsu Province (No. BK2009385).

References

1. Tak Y, Hong SJ, Lee JS, Yong K (2009) J Mater Chem 19(33):5945
2. Cao F–F, Wu X-L, Xin S, Guo Y-G, Wan L-J (2010) J Phys Chem C 114(22):10308
3. Jiang L-Y, Xin S, Wu X-L, Hong L, Guo Y-G, Wan L-J (2010) J Mater Chem 20(35):7565
4. Aldeek F, Balan L, Medjahdi G, Roques-Carmes T, Malval J-P, Mustin C, Ghanbaja J, Schneider Rl (2009) J Phys Chem C 113(45):19458
5. Hu Y, Liu Y, Qian H, Li Z, Chen J (2010) Langmuir 26(23):18570
6. Reiss P, Bleuse J, Pron A (2002) Nano Lett 2(7):781

7. Noh M, Kwon Y, Lee H, Cho J, Kim Y, Kim MG (2005) Chem Mater 17(8):1926
8. Lou XW, Chen JS, Chen P, Archer LA (2009) Chem Mater 21(13):2868
9. Li H, Shih WY, Shih W-H (2007) Ind Eng Chem Res 46(7):2013
10. Li J, Liu C-Y, Xie Z (2011) Mater Res Bull 46(5):743
11. Yang C, Liang G, Xu K, Gao P, Xu B (2009) J Mater Sci 44(7):1894. doi:10.1007/s10853-009-3247-8
12. Yang H, Holloway PH (2003) Appl Phys Lett 82(12):1965
13. Zhang J, Tang Y, Lee K, Ouyang M (2010) Science 327(5973):1634
14. Peng X, Schlamp MC, Kadavanich AV, Alivisatos AP (1997) J Am Chem Soc 119(30):7019
15. Nayak J, Sahu SN, Kasuya J, Nozaki S (2008) Appl Surf Sci 254(22):7215
16. Gorer S, Penner RM (1999) J Phys Chem B 103(28):5750
17. Zhang W-M, Wu X-L, Hu J-S, Guo Y-G, Wan L-J (2008) Adv Funct Mater 18(24):3941
18. Lin Y-S, Duh J-G, Hung M-H (2010) J Phys Chem C 114(30):13136
19. Datta A, Panda SK, Chaudhuri S (2007) J Phys Chem C 111(46):17260
20. Zhao D, He Z, Chan WH, Choi MMF (2008) J Phys Chem C 113(4):1293
21. Chen D, Zhao F, Qi H, Rutherford M, Peng X (2010) Chem Mater 22(4):1437
22. Fan D, Afzaal M, Mallik MA, Nguyen CQ, O'Brien P, Thomas PJ (2007) Coord Chem Rev 251(13–14):1878
23. Garje SS, Eisler DJ, Ritch JS, Afzaal M, O'Brien P, Chivers T (2006) J Am Chem Soc 128(10):3120
24. Cesar I, Kay A, Gonzalez Martinez JA, Grätzel M (2006) J Am Chem Soc 128(14):4582
25. Lee YH, Im SH, Rhee JH, Lee J-H, Seok SI (2010) ACS Appl Mater Interfaces 2(6):1648
26. Wang XF, Zhou Y, Xu JJ, Chen HY (2009) Adv Funct Mater 19(9):1444
27. Shalom M, Rühle S, Hod I, Yahav S, Zaban A (2009) J Am Chem Soc 131(29):9876
28. Lee HJ, Chen P, Moon S-J, Sauvage F, Sivula K, Bessho T, Gamelin DR, Comte P, Zakeeruddin SM, Seok SI, Grätzel M, Nazeeruddin MK (2009) Langmuir 25(13):7602
29. Park K, Yu H, Chung W, Kim B-J, Kim S (2009) J Mater Sci 44(16):4315. doi:10.1007/s10853-009-3641-2
30. Cao A, Liu Z, Chu S, Wu M, Ye Z, Cai Z, Chang Y, Wang S, Gong Q, Liu Y (2010) Adv Mater 22(1):103
31. Wang P, Jiang T, Zhu C, Zhai Y, Wang D, Dong S (2010) Nano Res 3(11):794
32. Cortes A, Svåsand E, Lavayen V, Segura R, Häberle P (2010) J Mater Sci 45(18):4958. doi:10.1007/s10853-010-4350-6
33. Banerji S, Byrne RE, Livingstone SE (1982) Transit Met Chem 7:5
34. Hart M (1975) Acta Crystallogr A 31(6):878
35. Zhai T, Fang X, Bando Y, Liao Q, Xu X, Zeng H, Ma Y, Yao J, Golberg D (2009) ACS Nano 3(4):949
36. Ferrari AC, Meyer JC, Scardaci V, Casiraghi C, Lazzeri M, Mauri F, Piscanec S, Jiang D, Novoselov KS, Roth S, Geim AK (2006) Phys Rev Lett 97(18):187401
37. Tong XL, Jiang DS, Liu ZM, Luo MZ, Li Y, Lu PX, Yang G, Long H (2008) Thin Solid Films 516(8):2003
38. Vemuri RS, Gullapalli SK, Zubia D, McClure JC, Ramana CV (2010) Chem Phys Lett 495(4–6):232
39. Nair MTS, Nair PK (1994) J Appl Phys 75(3):1557
40. Wang CL, Zhang H, Zhang JH, Li MJ, Han K, Yang B (2006) J Colloid Interface Sci 294(1):104
41. Spanhel L, Haase M, Weller H, Henglein A (1987) J Am Chem Soc 109(19):5649
42. Murray CB, Norris DJ, Bawendi MG (1993) J Am Chem Soc 115(19):8706
43. Stucky GD, Mac Dougall JE (1990) Science 247(4943):669